ELSEVIER

Contents lists available at ScienceDirect

Sensing and Bio-Sensing Research

journal homepage: www.elsevier.com/locate/sbsr





Green voltammetric strategy for sensitive determination of paracetamol in pharmaceuticals and serum using alizarin red S-modified glassy carbon electrodes

Wudneh Girum, Adane Kassa

Department of Chemistry, College of Natural and Computational Sciences, Debre Markos University, Debre Markos, P.O. Box 269, Ethiopia

ARTICLE INFO

Keywords: Paracetamol Glassy carbon electrode Alizarin red S Cyclic voltammetry Square wave voltammetry

ABSTRACT

This study introduces a highly sensitive electrochemical method for detecting paracetamol (PCT) in pharmaceutical tablets and human serum samples, utilizing a glassy carbon electrode modified with alizarin red S (poly (ARS)/GCE). PCT is one of the most widely used analgesic and antipyretic drugs; however, its overdose or prolonged use can lead to severe liver and kidney damage. Therefore, the development of sensitive and reliable methods for monitoring PCT levels in pharmaceutical formulations and biological fluids is crucial for ensuring drug safety and effective therapeutic monitoring. Characterization of the electrode confirmed that the surface modification with a conductive and electroactive polymer film (poly(ARS)) significantly enhanced the effective electrode surface area and reduced charge transfer resistance. Compared to the unmodified electrode, the modified electrode exhibited a well-resolved, irreversible redox peak at a significantly lower potential with a sixfold increase in current, highlighting the catalytic efficiency of the modifier toward PCT. The electrochemical behavior of PCT was analyzed via cyclic voltammetry and square wave voltammetry, revealing significantly enhanced sensitivity and selectivity due to the conductive polymer coating. Under optimized electrode condition square wave voltammetric current response of poly(ARS)/GCE showed linear dependence on concentration of $0.01\text{--}250.0~\mu\text{M}$ and an ultralow detection limit of 1.0~nM in phosphate buffer solution (pH 7.0). Analytical application on real samples confirmed the method's accuracy, achieving recovery rates of 98.8-100.3 % for pharmaceutical tablets and human blood serum, even in the presence of potential interferents. The developed method provides a cost-effective and robust alternative for PCT quantification, with superior performance compared to previously report electrochemical approaches.

1. Introduction

The analysis of pharmaceuticals plays a pivotal role in ensuring drug quality control and safeguarding public health. Paracetamol (*N*-acetyl-paminophenol), also known as acetaminophen (Scheme 1), is a widely used analgesic and antipyretic drug, commonly employed for relieving pain and reducing fever [1,2]. Despite its therapeutic benefits, excessive intake of PCT can lead to toxic effects such as hepatotoxicity and nephrotoxicity [2], underscoring the need for accurate monitoring of its concentration in pharmaceutical formulations and biological samples.

Analytical techniques are fundamental throughout a drug's lifecycle, from development to post-market surveillance, as they assess physical and chemical properties, inform dosage design, and ensure stability. Both quantitative and qualitative drug analyses are essential for

pharmacokinetic studies and quality assurance [3]. Given the extensive clinical use of paracetamol, reliable quantification methods for its analysis in drugs and biological fluids are crucial. Challenges in PCT determination include interference from impurities, degradation products, metabolites, or co-existing active substances, highlighting the need for selective, sensitive, and cost-effective methods for PCT detection in pharmaceutical and biological matrices [1,3].

A variety of analytical methods, such as chromatography [4,5], spectrophotometry [6,7], and spectrofluorometry [8,9], have been employed for PCT determination. However, these methods are often associated with extensive sample preparation, lengthy procedures, and high costs [10–13]. In contrast, electrochemical methods have gained attention as an efficient alternative due to their simplicity, rapid response, cost-effectiveness, and high sensitivity [1,10–13]. The

E-mail address: adane_kassa@dmu.edu.et (A. Kassa).

^{*} Corresponding author.

Scheme 1. Chemical structural of paracetamol

methods are increasingly preferred for analyzing real samples, offering vital insights into drug resistance and efficacy [14].

The use of chemically modified electrodes for the sensitive and selective detection of analytes is a notable advantage of electrochemical methods. Among these, carbon-based electrodes have gained significant attention in electroanalytical applications due to their affordability and versatility [15,16]. Glassy carbon electrodes are particularly popular for electrochemical analyses because of their excellent mechanical and electrical properties, broad potential range, and chemical stability. However, bare GCEs often face challenges such as limited sensitivity, selectivity, and surface fouling. To address these issues, modified GCEs have been developed to enhance electrochemical performance by increasing surface area, improving compatibility, and facilitating electron transfer, making them suitable for detecting biologically significant compounds.

This study aims to develop a green voltammetric method using an alizarin red S-modified GCE for the selective and sensitive detection of paracetamol in pharmaceutical formulations and human blood serum samples. The proposed method seeks to enhance the linear range, sensitivity, and detection limits, providing a reliable and efficient approach for pharmaceutical quality control and clinical applications.

2. Materials and methods

2.1. Chemicals and materials

All chemicals and reagents used in this study were of analytical grade and applied without further purification. Paracetamol (\geq 99.9 %) was sourced from Sigma Aldrich, while alizarin red S (\geq 99.7 %) was obtained from Samir Tech-Chem. (p) Ltd. Potassium hexacyanoferrice(III) (98.0 %) and potassium hexacyanoferrate(II) (98.0 %) were supplied by BDH Laboratories. Additional chemicals included potassium chloride (99.5 %), sodium monohydrogen phosphate (\geq 98.0 %), and sodium dihydrogen phosphate (\geq 98.0 %), all procured from Blulux Laboratories. Hydrochloric acid (37.0 %) and nitric acid (70.0 %) were purchased from Fisher Scientific, while sodium hydroxide (Extra pure) was acquired from Lab Tech Chemicals.

The instruments utilized in this study included an electronic balance (Nimbus, ADAM Equipment, USA), a refrigerator (Lec Refrigeration PLC, England), a deionizer/distiller (Evoqua Water Technologies), and a centrifuge (1020D, Centurion Scientific LTD, UK). Additionally, the CHI 760E potentiostat (Austin, Texas, USA), a pH meter (8000 CE, Romania), and a Basi potentiostat (USA) were used for experimental analyses.

2.2. Procedure

2.2.1. Preparation of poly(ARS)/GCE

Initially, the bare GCE was polished using a micro-cloth with alumina powders of 0.1 μM and subsequently 0.05 μM particle size. After polishing, the electrode was thoroughly rinsed with distilled water. The cleaned GCE was then immersed in a 0.1 M phosphate buffer solution (PBS) at pH 7.0 containing 1.0 mM ARS. The potential was cycled between -0.8 V and + 1.8 V for 10 cycles at a scan rate of 100 mV s $^{-1}$. To remove any physically adsorbed monomer species, the poly(ARS)/GCE was rinsed again with distilled water. The modified electrode was then stabilized in 0.5 M H_2SO_4 by scanning between -0.8 V and + 0.8 V until

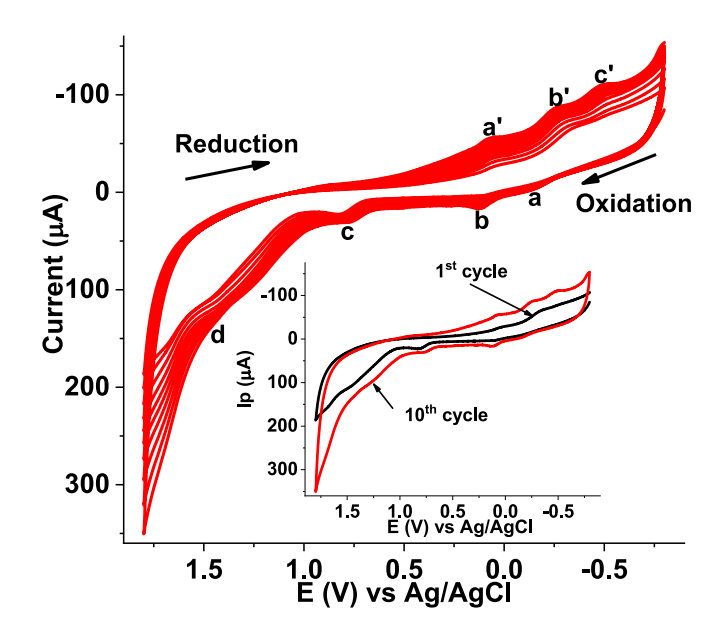


Fig. 1. Repetitive CVs of GCE in pH 7.0 PBS containing 1.0 mM ARS scanned between -0.8 & +1.8 V at a scan rate of 100 mV s⁻¹ for 10 cycles. Inset: CVs 1st cycle, and 10th cycle of poly(ARS)/GCE.

a stable cyclic voltammogram was achieved. Finally, the stabilized poly (ARS)/GCE was air-dried before being used in further experiments.

2.2.2. Preparation of standard PCT solution

A stock solution of paracetamol with a concentration of $10.0 \, \text{mM}$ was prepared by dissolving $0.03779 \, \text{g}$ of PCT in $100 \, \text{mL}$ of distilled water. From this stock solution, working standard solutions were prepared through serial dilutions using PBS adjusted to the desired pH levels.

2.2.3. Preparation of real samples

2.2.3.1. Tablet sample. Tablets from four brands Epharm (Ethiopian Pharmaceuticals Manufacturing Factory, Ethiopia), Corova (Aden Healthcare, India), Para-Denk (Germany), and Panadol (GlaxoSmithK-line plc, Ireland) were obtained from a local pharmacy in Bahir Dar, Ethiopia. Five tablets from each brand were randomly selected, ground, and homogenized using a mortar and pestle. A stock solution with a nominal concentration of 2.0 mM was prepared for each brand by dissolving an amount of tablet powder equivalent to 30.2 mg of PCT in 100 mL of distilled water in a volumetric flask. Further working solutions for each brand were prepared by serial dilution of the stock solution using PBS at pH 7.0. For spike and interference studies, working tablet solutions were also spiked with standard PCT solutions following the same procedure.

2.2.3.2. Human blood serum sample. A 1.0 mL serum sample for PCT analysis was obtained from human blood serum collected at Tibebe Gion Referral Hospital in Bahir Dar City, Ethiopia. The serum was transferred to a 25 mL conical flask, then filled to the mark with PBS at pH 7.0 and stored in refrigeration for subsequent analysis. For recovery studies, the serum samples were spiked with a standard PCT solution.

3. Results and discussion

3.1. Fabrication of poly(ARS)/GCE

The poly(ARS)/GCE was prepared by scanning the potential of a polished GCE in a 1.0 mM ARS monomer solution with 0.1 M PBS at pH 7.0, within a potential range of -0.8 to +1.8 V for 10 cycles at a scan rate of 100 mV s⁻¹ (Fig. 1). The resulting cyclic voltammogram showed

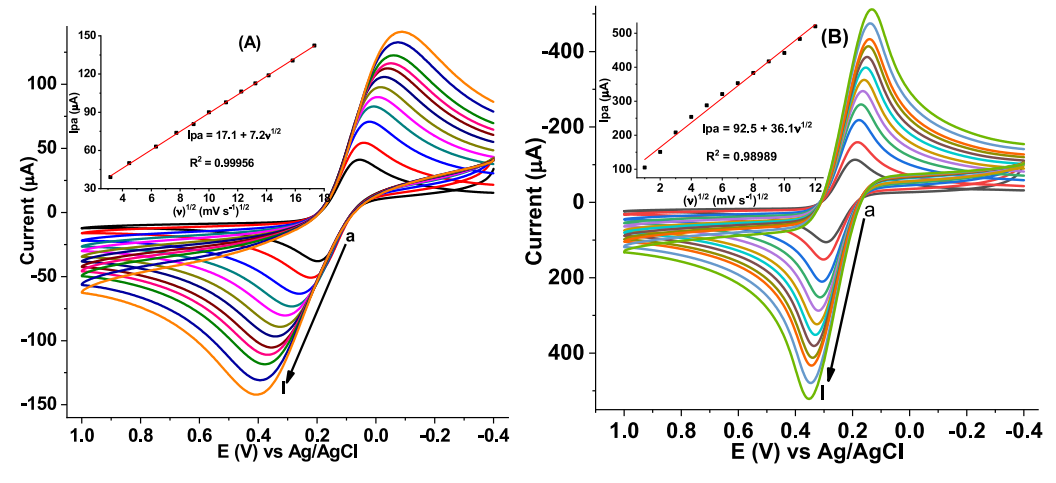


Fig. 2. CVs of bare GCE (A), and poly(ARS)/GCE (B) in pH 7.0 PBS containing 10.0 mM Fe(CN) $_6^{3-/4-}$ and 0.1 M KCl at (a–l: 10, 20, 40, 60, 80, 100, 125, 150, 175, 200, 250, and 300 mV s⁻¹, respectively). Inset: plot of I_{pa} vs. square root of scan rate.

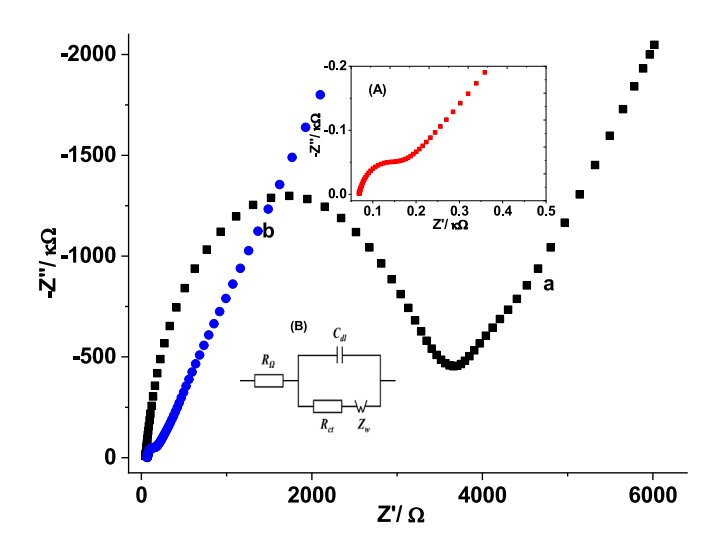


Fig. 3. Nyquist plot of (a) bare GCE and (b) poly(ARS)/GCE in pH 7.0 PBS containing 10.0 mM [Fe(CN)6]^{3-/4-} and 0.1 M KCl, measured over a frequency range of 0.01–100,000 Hz, with an amplitude of 0.01 V and potential of 0.23 V. Inset: (A) zoomed of curve b, and (B) proposed equivalent circuit.

the development of anodic peaks (a-d) and cathodic peaks (a'-c') with increasing current, indicating the formation of an electroactive polymer film on the electrode surface. Compared to the first cycle (Inset of Fig. 1), where a broad anodic peak and a wide cathodic peak were observed, the 10th cycle revealed more defined anodic peaks (b and c), including a newly formed peak (b) and a cathodic peak (c'). This was accompanied by a significant increase in current and a shift in the potential toward more positive values, indicating the successful deposition of the redox polymer film on the electrode.

3.2. Cyclic Voltammetric characterization of poly(ARS)/GCE

To evaluate how surface modification affects the electrode's surface area, cyclic voltammograms of $\mathrm{Fe(CN)_6}^{3-}/^{4-}$ were obtained for both the unmodified and poly(ARS)-modified GCEs (Fig. 2) across various scan rates. The active surface areas of the electrodes were calculated using the Randles–Ševčík equation (Eq. (1)) [17], by determining the slope from the plot of anodic peak current against the square root of the scan rate.

$$I_{pa} = 2.69 \times 10^{5} n^{3/2} A D^{1/2} \nu^{1/2} C_{o}$$
 (1)

 Table 1

 Summary of calculated circuit elements for the studied electrodes.

Electrode	$R_{\rm s}/\Omega$ cm ²	$R_{\rm ct}/\Omega$ cm ²	f/Hz	C _{dl} /F	k ^o
GCE (curve a)	14.1	4290.7	316.2	1.8×10^{-7}	7.8×10^{-8}
poly(ARS) (curve b)	14.1	192.6	55.2	$\begin{array}{c} 1.5 \times \\ 10^{-5} \end{array}$	$\begin{array}{c} 3.5 \times \\ 10^{-7} \end{array}$

Here, Ipa represents the anodic peak current, n is the number of electrons involved in the transfer process (n=1), A denotes the active surface area of the electrode, D is the diffusion coefficient of Fe(CN) $_{6}^{3-/}$ (D = $7.6 \times 10^{-6} \ cm^{2} s^{-1}$), C_{0} refers to the bulk concentration of the redox probe ($C_{0}=10.0 \ mM$), and ν is the scan rate.

Compared to the unmodified GCE with an effective surface area of $0.09~{\rm cm}^2$, the poly(ARS)/GCE exhibited a fivefold increase in effective surface area, reaching $0.45~{\rm cm}^2$. The improvement is ascribed to the electrode surface modification with the conductive polymer film, which significantly increased the active surface area. Consequently, the rise in peak current observed for the probe in Fig. 2 using the poly(ARS)/GCE is directly linked to this enhanced surface area.

3.3. Electrochemical impedance spectroscopic characterization

Electrochemical impedance spectroscopy was employed to confirm the surface modification and assess the conductive properties of the modifiers. Fig. 3 shows the Nyquist plots for bare GCE and poly(ARS)/GCE modified electrodes. As observed, all electrodes displayed a semicircle in the high-frequency region and a straight line in the low-frequency region, which corresponds to the diffusion of electroactive species from the bulk solution to the solution-electrode interface. This behavior is consistent with the recommended equivalent circuit (Inset R)

$$C_{dI} = \frac{1}{2\pi P_{eff}} \tag{2}$$

Where Cdl represents the double-layer capacitance, f is the frequency corresponding to the maximum value of the imaginary resistance, and Rct is the charge transfer resistance. The circuit elements, including Rs, Rct, and Cdl, for each electrode studied, were calculated from the respective Nyquist plot using Eq. (1). The apparent heterogeneous electron transfer rate constant (ko) was calculated using Eq. (2) [18]. These values are summarized in Table 1.

Among the two electrodes, the poly(ARS)/GCE exhibited the lowest

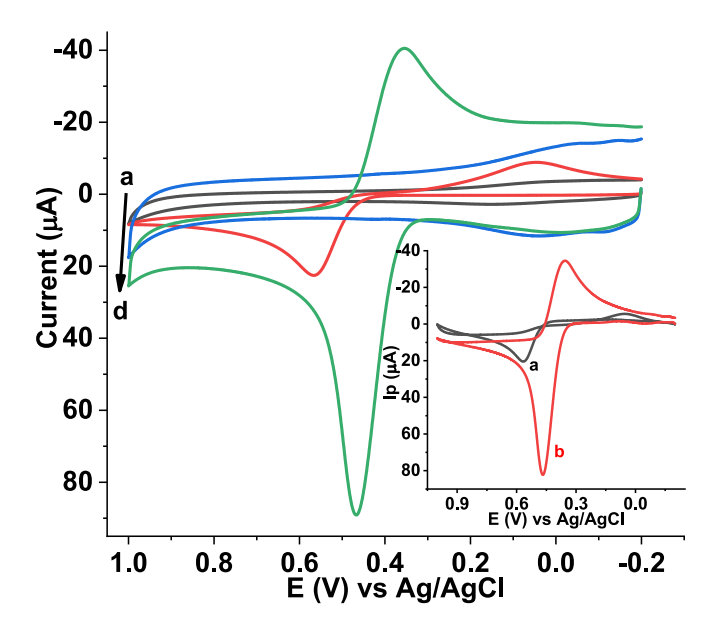


Fig. 4. Cyclic voltammograms of bare (a & b) and poly(ARS)/GCE (c & d) in pH 7.0 PBS with no PCT (a & c) and 1.0 mM PCT (b & d) at a scan rate of 100 mV s $^{-1}$. Inset: Blank-corrected cyclic voltammograms of (a) bare GCE and (b) poly(ARS)/GCE.

Rct value (192.6 Ω , curve b of Fig. 3) (Table 1), indicating that the poly (ARS) film significantly enhanced the conductivity and, consequently, the electron transfer rate between the substrate and the analyte. This improvement can be attributed to the conductive properties of the polymer film. The apparent heterogeneous electron transfer rate constant (k^0) value was estimated by using Eq. (3).

$$k^0 = \frac{RT}{F^2 A C R_{ct}} \tag{3}$$

Where R– the molar gas constant, T– temperature, F– Faraday constant, A– surface area of the electrode, and C– the concentration of ${\rm [Fe(CN)_6]}^{3-/4}$.

As shown in Table 1, the poly(ARS)/GCE exhibits a k° value 4.5 times higher than that of the unmodified GCE, clearly demonstrating the electrocatalytic properties of the modified electrode toward the probe. The surface roughness factor (RF), which reflects the increase in surface area, was further calculated for poly(ARS)/GCE using Eq. (4).

$$R_F = \frac{C_{dl}}{C_S} \tag{4}$$

Where R_F represents the surface roughness, and $C_{\rm dl}$ and C_s are the electrochemical double-layer capacitances of a planar, smooth electrode surface of the same material, measured under identical conditions. The RF value of poly(ARS)/GCE is five times greater than that of the unmodified GCE, which aligns with the slopes observed for the two electrodes (Fig. 2 (A & B, respectively)) and, consequently, the surface area.

3.4. Cyclic voltammetric investigation of PCT

3.4.1. Electrochemical behavior of PCT at poly(ARS)/GCE

In this study, the electrochemical oxidation of paracetamol was investigated using cyclic voltammetry and square wave voltammetry. The poly(ARS)/GCE exhibited low charge transfer resistance (Rct), high surface roughness, and an enhanced effective surface area, indicating its catalytic role. The electrochemical behavior of PCT showed irreversible oxidation and reduction peaks at both unmodified and modified GCEs, with differences in current intensity and peak potential (Fig. 4). The appearance of a well-defined oxidative and reductive peak at a significantly reduced potential ($\Delta E = 188 \text{ mV}$) and a more than sixfold

increase in current at poly(ARS)/GCE (curve b of inset) compared to the unmodified GCE (curve a of inset) confirmed the catalytic effect of the poly(ARS) film on PCT. The improved potential and current response at poly(ARS)/GCE demonstrate its suitability for the determination of PCT in real samples.

3.4.2. Effect of scan rate on peak current and peak potential

The effect of different scan rates on the electrochemical response of paracetamol at poly(ARS)/GCE was examined using cyclic voltammetry. Fig. 5 shows the cyclic voltammogram of PCT in pH 7.0 PBS at varying scan rates. The observed shift of the peak potential in the positive direction with increasing scan rate (Fig. 5) confirms the irreversible nature of PCT oxidation at poly(ARS)/GCE. The linear relationship between peak current and scan rate yielded a determination coefficient (R^2) of 0.97288 (Fig. 5B). However, a stronger correlation was found between peak current and the square root of scan rate ($R^2 = 0.99745$) (Fig. 5C), suggesting that the oxidation of PCT at the poly(ARS)-modified electrode is primarily diffusion-controlled [19,20]. The slope of 0.64 for the log(Ip) versus $log(\nu)$ plot (Fig. 5D), which is close to the theoretical value of 0.50 for a purely diffusion-controlled reaction, further supports the conclusion that PCT oxidation at poly(ARS)/GCE is predominantly diffusion-controlled [20].

The kinetic parameters, including the number of electrons involved and the electron transfer coefficient for the oxidation of PCT at poly (ARS)/GCE, were calculated. The αn value in Eq. (5) for the irreversible oxidation was determined by analyzing the cyclic voltammogram of PCT in pH 7.0 PBS at a scan rate of 100 mV s⁻¹, as shown in Fig. 5A. The relationship between Ep and $\ln \nu$ for an irreversible process follows Eq. (6) [17].

$$E_p - E_{p\frac{1}{2}} = {}^{48}\!/_{\alpha n}$$
 (5)

$$Ep = E^{\circ} + \frac{RT}{(1-\alpha)nF} \left\{ 0.780 + ln \left(\frac{D_R^{\frac{1}{2}}}{k^{\circ}} \right) + ln \left[\frac{(1-\alpha)nF\nu}{RT} \right]^{\frac{1}{2}} \right\}$$
 (6)

In this context, α represents the charge transfer coefficient, n is the number of electrons transferred, Ep is the peak potential, E^0 is the formal potential, E^0 is the electrochemical rate constant, and the other parameters are defined by standard electrochemical theory.

From the cyclic voltammogram of PCT at a scan rate of 100 mV s^{-1} (Fig. 5), the peak potential (Ep) and half-peak potential (Ep_{1/2}) were found to be 468 mV and 420 mV, respectively. Using these values, α n product was determined to be 1.0, assuming that α for a completely irreversible electrode process is 0.50 [20]. This indicates that two electrons (n=2) are involved in the electro-oxidation of PCT at the poly (ARS)/GCE surface. Additionally, from the slope of 0.02 in the fitted line (Epa (V) = 0.40 + 0.02ln ν) in the plot of Ep versus ln(ν) (Fig. 5E), the value of n($1-\alpha$) was calculated to be 0.64 at 25 °C using Eq. (6). Given that two electrons are involved in the oxidation of PCT, the electron transfer coefficient (α) was estimated to be 0.68, further supporting the irreversibility of the PCT oxidation process [17,18,20].

3.4.3. Effect of solution pH

To optimize the poly(ARS)/GCE response for PCT oxidation, the impact of pH on electrochemical oxidation was examined using cyclic voltammetry across a pH range of 3.0–9.0 in a phosphate buffer solution containing 1.0 mM PCT, at a scan rate of 100 mV s⁻¹ (Fig. 6). The observed shift of the potential toward more negative values with increasing pH (Fig. 6A) suggests the involvement of protons during PCT oxidation at poly(ARS)/GCE. The slope of 0.05 V for the plot of oxidative peak potential versus pH (curve b of Fig. 6B) indicates a 1:1 ratio of proton and electron involvement [18].

Additionally, the PCT current at poly(ARS)/GCE increased as the pH ranged from 4.0 to 7.0, then decreased at pH values above 7.0 (curve a of Fig. 6B), with pH 7.0 identified as the optimal value. This trend may be due to electrostatic interactions between PCT (pKa 9.5) [21] and alizarin

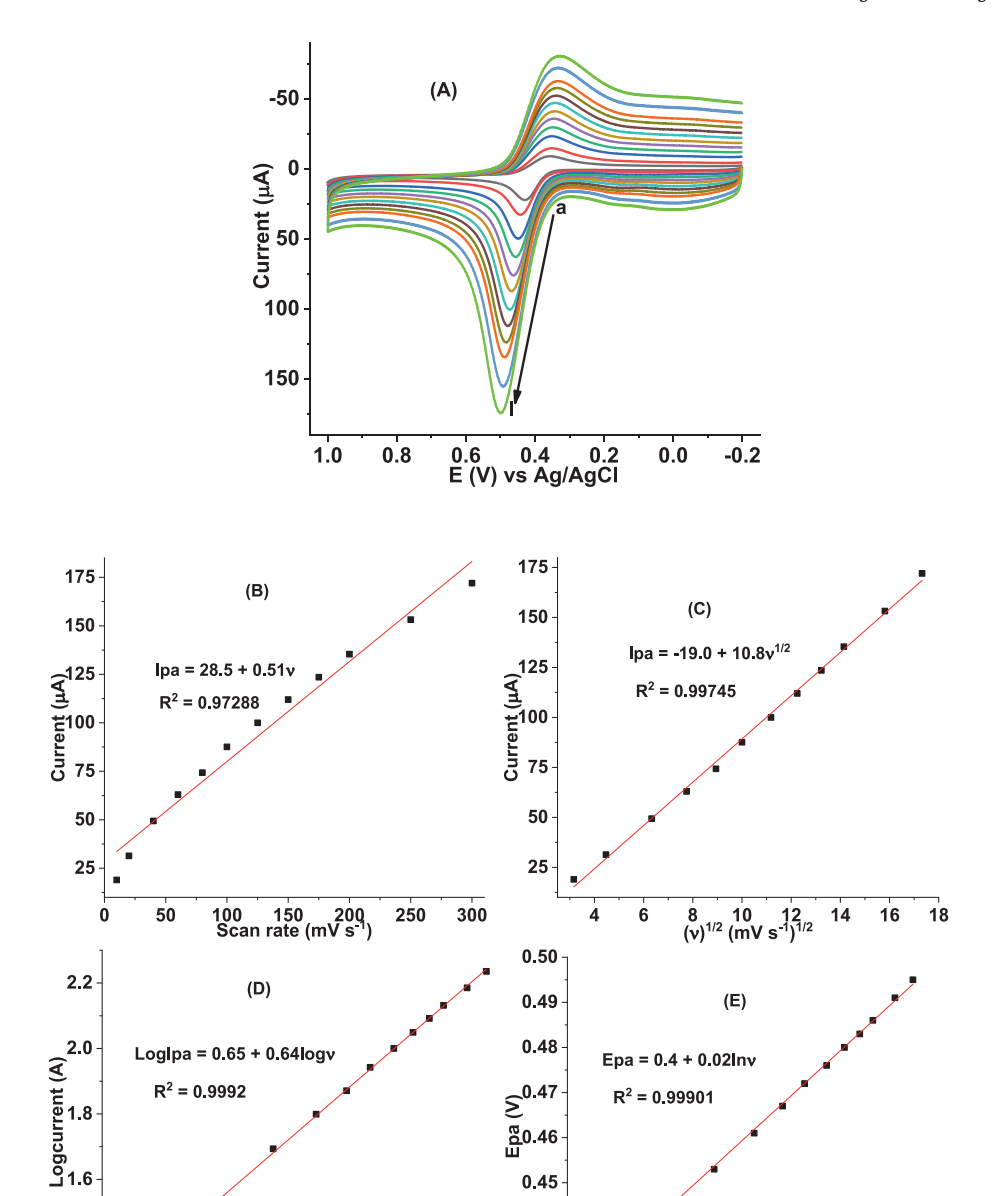


Fig. 5. (A) Cyclic voltammograms of poly(ARS)/GCE in 1.0 mM PCT (pH 7.0 PBS) at various scan rates (a–l: 10, 20, 40, 60, 80, 100, 125, 150, 175, 200, 250, and 300 mV s⁻¹, respectively), (B) plot of peak current (Ip) versus scan rate (ν), (C) plot of Ip versus scan rate, (D) plot of log(Ip) versus log(ν), and (E) plot of peak potential (Ep) versus ln(ν).

2.4

1.5 1.8 2.1 Logscan rate (V s 1) 0.44

0.43

2.5

red S has two pKa values (pKa 5.49 and 10.85) [22]. The increase in current from pH 4.0 to 6.0 may result from the attraction between deprotonated PCT and protonated alizarin red S. At pH values between 3.0 and 6.0, lower oxidation peak currents were observed, likely due to PCT hydrolysis and the involvement of $\rm H^+$ in the formation of the unstable oxidation product, NAPQI. At pH levels above 7.0, the participation of $\rm OH^-$ destabilized NAPQI, further reducing the peak current.

1.4

0.9

1.2

A reaction mechanism was proposed (Scheme 2) based on the determined kinetic parameters (nnn and $\alpha \setminus A$) and the observed 1:1 proton-to-electron ratio. This mechanism aligns with findings reported in earlier studies [23].

3.5. Square wave voltammetry investigation of PCT using poly(ARS)/GCE

Square wave voltammetry (SWV) is a more effective technique than cyclic voltammetry, offering higher sensitivity, better resolution, and lower detection limits [18,24]. SWV was therefore used for the quantitative analysis of PCT in tablet and serum samples. Fig. 7 illustrates the SWV responses of 1.0 mM PCT in PBS (pH 7.0) at both bare and poly (ARS)/GCE electrodes. At the bare glassy carbon electrode, the poor electroactivity of PCT resulted in weak and insignificant current peaks. However, at the poly(ARS)/GCE, a well-defined anodic peak and a reduction in overpotential were observed for PCT, demonstrating that accurate determination of PCT is feasible using SWV with the poly (ARS)/GCE surface.

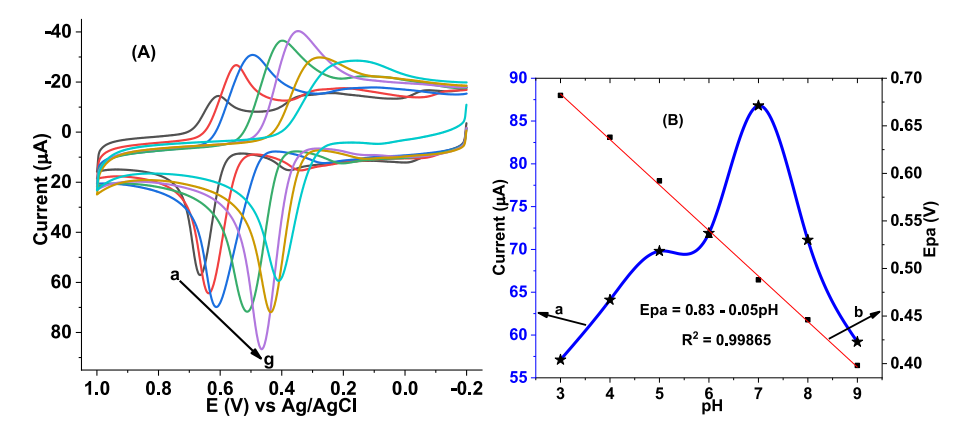


Fig. 6. (A) CVs of 1.0 mM PCT in PBS at various pH values (a-g: 3.0, 4.0, 5.0, 6.0, 7.0, 8.0, and 9.0, respectively), (B) mean \pm SD of peak (a) current and (b) potential plotted against pH across the entire pH range.

Scheme 2. Proposed reaction mechanism for PCT.

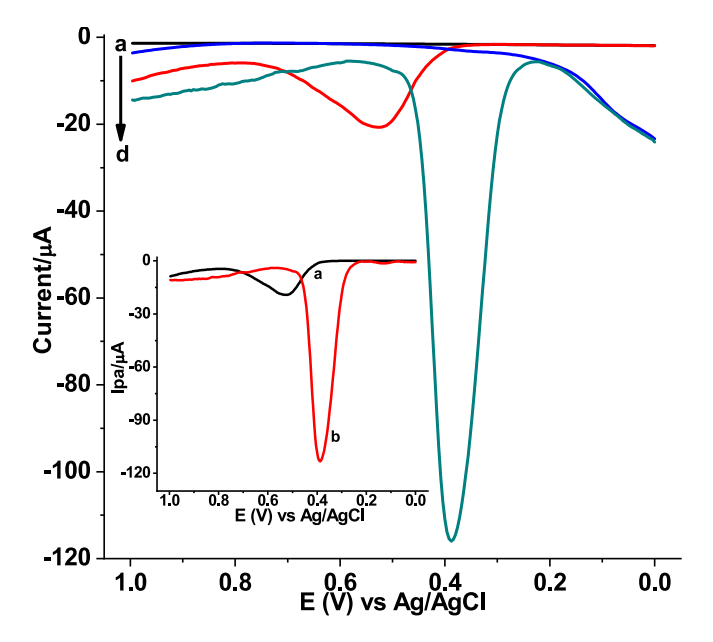


Fig. 7. SWVs of bare GCE (a & b) and poly(ARS)/GCE (c & d) in pH 7.0 PBS with and without 1.0 mM PCT (a & c: without PCT, b & d: with PCT) at a potential increment of 4 mV, amplitude of 25 mV, and frequency of 15 Hz. Inset: Background corrected SWVs of PCT at (a) bare GCE and (b) poly (ARS)/GCE.

3.5.1. Square wave voltammetric parameter optimization

To optimize the square wave voltammetry parameters, step potential, amplitude, and frequency were systematically evaluated. The results showed that the peak current increased with higher step potential, amplitude, and square wave frequency, accompanied by a rise in capacitive current (Fig. 8A-C). Based on these observations, the optimal parameters were determined to be a step potential of 6 mV, amplitude of 35 mV, and a square wave frequency of 20 Hz for further analysis.

3.6. Calibration curve and method detection limit

Fig. 9 displays the square wave voltammograms for different concentrations of PCT under optimized solution conditions and method parameters. The average current response (n=3) showed a linear correlation with PCT concentration within the range of $0.01-250.0~\mu M$. The method achieved a limit of detection (LoD) of 1.0~n M (calculated as 3~s/m, n=7) and a limit of quantification (LoQ) of 3.4~n M, as shown in the inset of Fig. 9. The %RSD values for triplicate measurements were all below 3.0~%, confirming the method's high precision when employing the conductive polymer ARS as an electrode modifier.

The high sensitivity (calculated as the slope value of the calibration plot divided by the surface area) approaching 1.0 validates the accuracy and significance of the developed method.

3.7. Analytical application of the poly(ARS)/GCE

3.7.1. Tablet formulation samples

To evaluate the PCT content in tablet samples and compare it to the nominal values provided by the manufacturers, samples from four brands (EPHARM, Corova, Para-Denk, and Panadol) were prepared following the outlined experimental procedure. The square wave voltammograms for tablets with nominal PCT concentrations of 20.0 and 40.0 μM for each brand are presented in Fig. 10. The measured currents were used to determine the PCT concentration in each tablet, and the results were compared to the labeled values (Table 2). As indicated in the table, the measured PCT content ranged between 98.8 % and 100.0 % of the expected values, with %RSD values below 3.3 %. These results confirm the method's accuracy and precision, highlighting its suitability for determining PCT in complex matrices.

3.7.2. Human blood serum sample

As shown in Fig. 11A, the absence of a peak at the characteristic potential of PCT confirmed that PCT was not present in the analyzed human blood serum sample. However, in Fig. 11B-D, a peak appeared at a different potential, which was identified as "a" for uric acid and "c" for creatinine [18].

3.8. Validation of the developed method

3.8.1. Spike recovery study

3.8.1.1. Human blood serum sample. As illustrated in Fig. 11, the currents for peaks (a and c) in the unspiked serum sample remained consistent, even with increasing concentrations of spiked PCT, suggesting that these peaks are unrelated to PCT. Conversely, a new peak (peak b in curves B—D) emerged, showing a rising current response

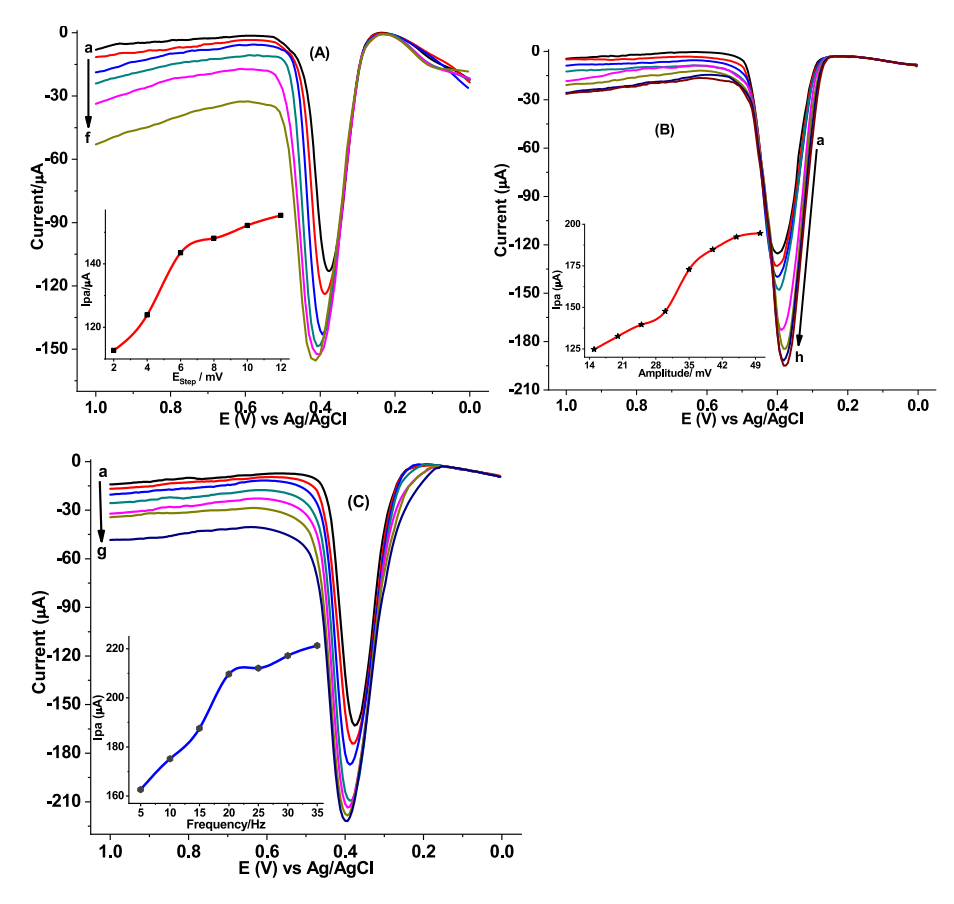


Fig. 8. SWVs of poly(ARS)/GCE in pH 7.0 PBS containing 1.0 mM PCT under optimized parameters: (A) step potential (a-f: 2, 4, 6, 8, 10, and 12 mV) with a fixed amplitude of 25 mV and frequency of 15 Hz; (B) amplitude (a-h: 15, 20, 25, 30, 35, 40, 45, and 50 mV) with a step potential of 6 mV and frequency of 15 Hz; and (C) frequency (a-g: 5, 10, 15, 20, 25, 30, and 35 Hz) with a step potential of 6 mV and amplitude of 35 mV. Insets show the corresponding plots of peak current (Ip) versus (A) step potential, (B) amplitude, and (C) frequency.

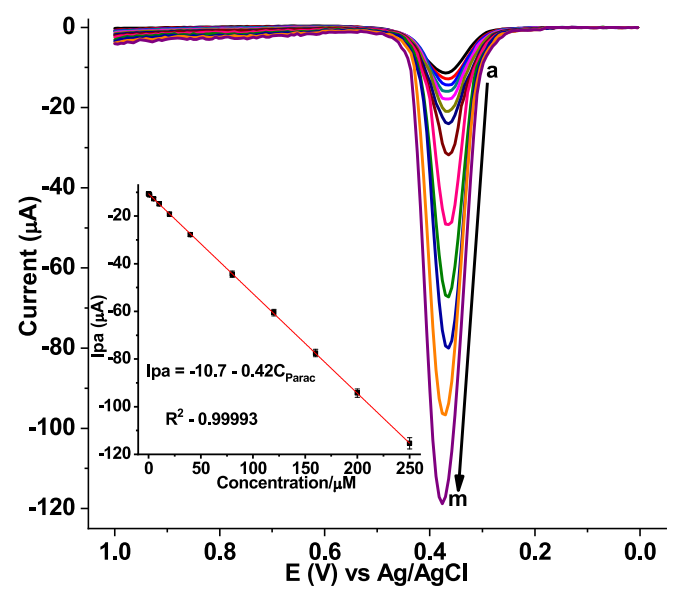


Fig. 9. Blank corrected SWVs of poly(ARS)/GCE in pH 7.0 PBS for different concentrations of PCT (a–m: 0.01, 0.05, 0.5, 1.0, 5.0, 10.0, 20.0, 40.0, 80.0, 120, 160, 200.0, and 250.0 μM , respectively) at step potential 6 mV, amplitude 35 mV, and frequency 20 Hz. Inset: plot of oxidative peak current (mean \pm % RSD as error bar) vs. concentration of PCT.

proportional to the spiked PCT levels. The spike recovery results,

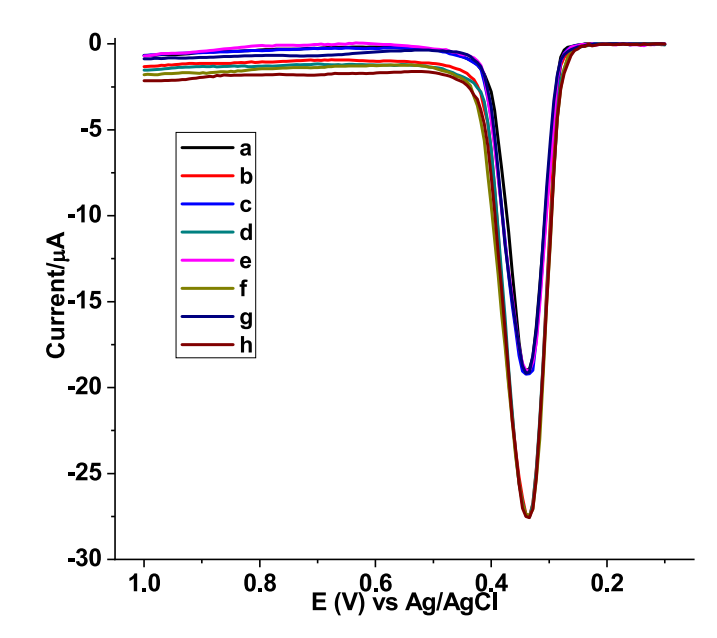


Fig. 10. Blank corrected SWVs of poly(ARS)/GCE in pH 7.0 PBS containing (A) 20.0 and (B) 40.0 μ M, PCT tablet samples of different brands (a & b: EPHARM, c & d: Corova, e & f: Para-Denk, and g & h: Panadol, respectively).

summarized in Table 3, ranged between 99.75 % and 100.30 %, with a %RSD below 3.2 % for PCT in human serum samples. These results confirm the method's accuracy and reliability for quantifying PCT in

Table 2Summary of detected PCT content and percent detected as compared to the nominal value for each analyzed tablet brand.

Tablet brand	Labeled	Nominal PCT	Detected P	Detected PCT in	
	PCT (mg/ tablet)	in sample (μM)	sample (μM) ^a	tablet (mg/ tablet)	PCT (%)
EPHARM	500	20.0	19.76 ± 0.030	494.0	98.8
		40.0	$\begin{array}{c} 39.67 \pm \\ 0.020 \end{array}$	495.9	99.20
Corova	500	20.0	$\begin{array}{c} 20.0 \pm \\ 0.017 \end{array}$	500.0	100.0
		40.0	$\begin{array}{c} 40.0 \; \pm \\ 0.015 \end{array}$	500.0	100.0
Para- Denk	500	20.0	$19.88 \pm \\ 0.025$	497.0	99.4
		40.0	$\begin{array}{c} 39.86 \pm \\ 0.021 \end{array}$	498.3	99.65
Panadol	500	20.0	$19.95 \pm \\ 0.033$	498.8	99.75
		40.0	$\begin{array}{c} 39.95 \; \pm \\ 0.020 \end{array}$	499.4	99.88

 $^{^{\}mathrm{a}}$ Detected mean PCT \pm %RSD.

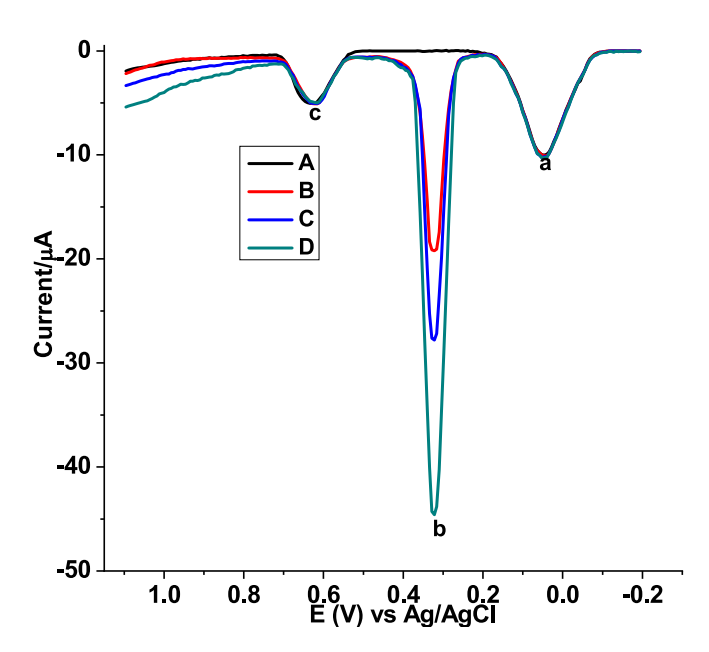


Fig. 11. Background-corrected SWVs of poly(ARS)/GCE in pH 7.0 PBS with (A–D: unspiked human blood serum sample, serum spiked with 20.0 μ M, 40.0 μ M, and 80.0 μ M PCT, respectively). Peaks correspond to (a) uric acid, (b) PCT, and (c) creatinine.

Table 3 Recovery of 20.0, 40.0, and 80.0 μ M PCT in spiked human blood serum samples.

Sample	PCT before spike (μM)	Added PCT (μM)	Found PCT (μM) ^a	Recovery (%) ^b
В	ND	20.0	19.95 ± 0.030	99.75 ± 3.00
C	ND	40.0	40.0 ± 0.022	100.00 \pm
				2.20
D	ND	80.0	80.23 ± 0.032	100.3 ± 3.20

ND not detected.

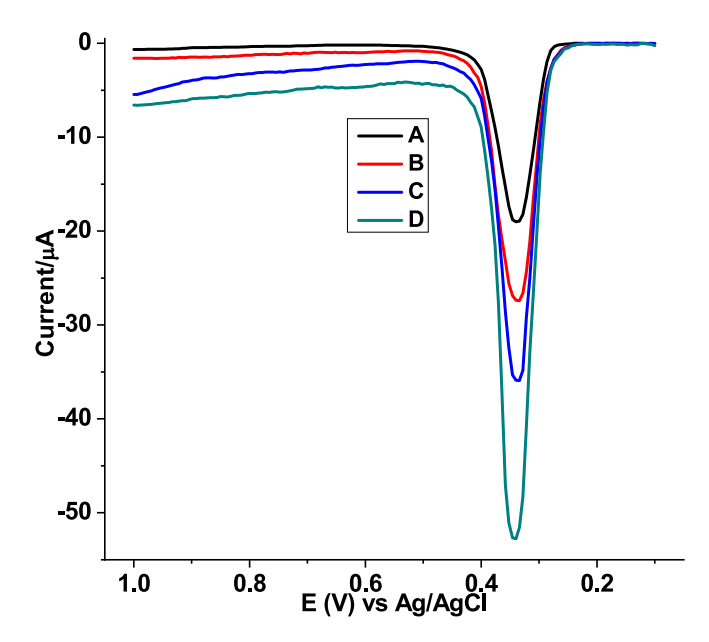


Fig. 12. Background-subtracted SWVs of poly(ARS)/GCE in pH 7.0 PBS with Epharm brand tablet samples spiked with standard PCT at concentrations of 0.0, 20.0, 40.0, and 80.0 μ M (A–D, respectively).

Table 4 Summary of spike recovery results for 20.0, 40.0, and 80.0 μ M PCT added to tablet solutions with a PCT concentration of 19.76 \pm 0.03 μ M.

Spiked PCT (μM)	Expected PCT (μM)	Detected PCT (mean \pm RSD) (μ M) a	Recovery (%)
	19.76	19.76 ± 0.03	_
20.00	39.76	39.64 ± 0.02	99.4
40.00	59.76	59.76 ± 0.025	100.0
80.00	99.76	100.0 ± 0.03	100.3

 $^{^{\}rm a}$ Detected mean PCT \pm RSD.

human blood serum.

3.8.1.2. Tablet formulation sample. To further confirm the applicability of the developed method for PCT determination in real samples, where matrix effects might be significant, spike recovery experiments were conducted. The Epharm brand tablet sample, previously analyzed, was spiked with standard PCT solutions at concentrations of 0.0, 20.0, 40.0, and $80.0~\mu$ M. Fig. 12 shows the square wave voltammograms of the Epharm tablet sample spiked with different PCT concentrations. The spike recovery results, ranging from 99.4~% to 100.3~% (Table 4), demonstrated the accuracy of the method and validated the use of the poly(ARS)/GCE method for PCT determination in real samples.

3.8.1.3. Interference study. The proposed method's selectivity for detecting PCT was assessed in the presence of various potential interferents. Substances were selected based on their possible inclusion in PCT tablets, structural similarity to PCT, or likelihood of being coadministered. The effect of each interferent was tested at varying concentrations (Fig. 13). As summarized in Table 5, the presence of these interferents in tablet samples containing a fixed PCT concentration caused random errors, all within an acceptable tolerance of ± 5 %, confirming the method's selectivity.

3.8.1.4. Stability study. The %RSD for five consecutive measurements of the PCT current at poly(ARS)/GCE, taken every two hours within a single day (Fig. 14A), and for similar measurements taken every four days over a span of twenty days (Fig. 14B), were 1.82 % and 3.33 %, respectively. These results, obtained with a constant concentration of

 $^{^{\}mathrm{a}}$ Detected mean PCT \pm RSD.

 $^{^{\}rm b}\,$ % Recovery PCT \pm %RSD.

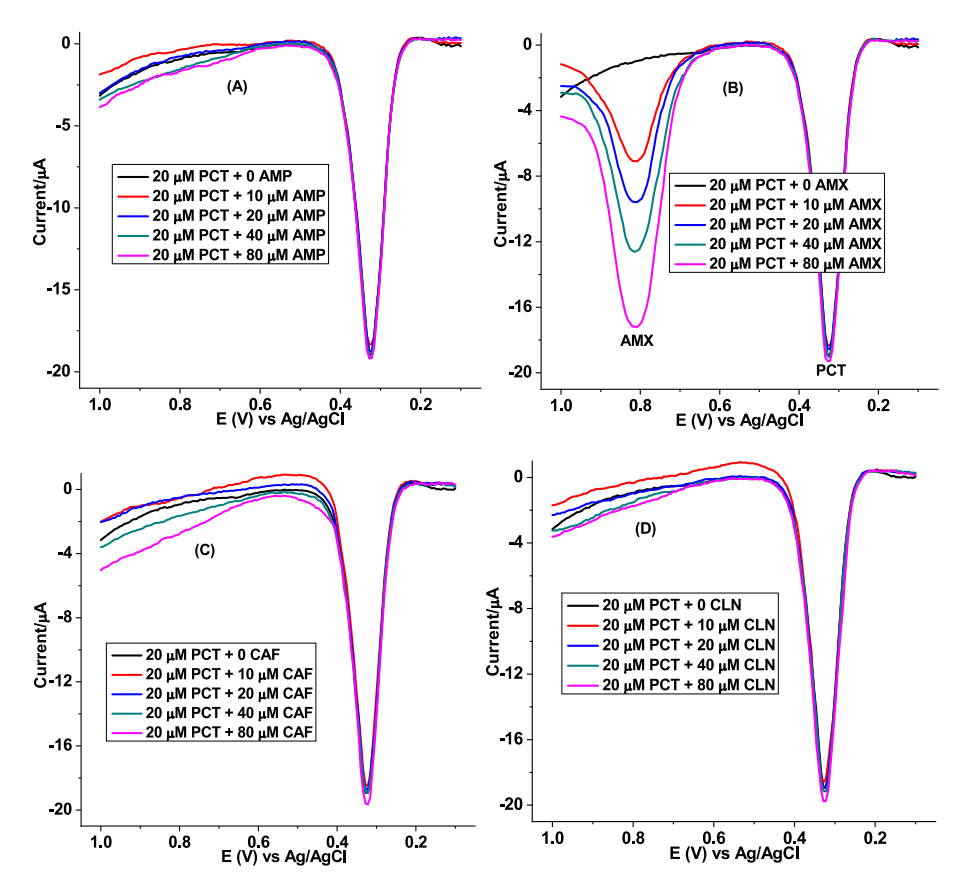


Fig. 13. Background corrected SWVs of $20.0~\mu M$ PCT tablet solution (pH 7.0 PBS) in the presence of (A) AMP, (B) AMX, (C) CAF, and (D) CLN at their various concentrations (0.0, 10.0, 20.0, 40.0, & 80.0 μM).

Table 5 Summary of recovery of 20.0 μ M PCT in tablet sample in the presence of AMP, AMX, CAF, and CLN at their levels from 0.0 to 80.0 μ M.

Interferent type	Interferent added (µM)	Detected current (mean for n 3) (µA)	Expected current (mean for n 3) (µA)	% error
	0.0	19.0	19.0	
	10.0	18.4	19.0	3.3
AMP	20.0	18.8	19.0	1.06
	40.0	19.0	19.0	0.0
	80.0	19.2	19.0	1.05
	0.0	19.0	19.0	
	10.0	18.3	19.0	3.8
A 3 #37	20.0	18.6	19.0	2.1
AMX	40.0	19.0	19.0	0.0
	80.0	19.3	19.0	1.6
	0	19.0	19.0	
	10.0	18.5	19.0	2.7
CAE	20.0	18.8	19.0	1.06
CAF	40.0	18.9	19.0	0.5
	80.0	19.6	19.0	3.1
	0	19.0	19.0	
	10.0	18.6	19.0	2.1
OI N	20.0	18.9	19.0	0.5
CLN	40.0	19.2	19.0	1.05
	80.0	19.7	19.0	3.7

PCT, demonstrate the stability of the polymer film.

The excellent spike recovery, interference recovery, and stability, combined with a wide linear range and low limit of detection, confirmed the effectiveness of the developed method for determining PCT in real-world samples, including those with complex matrices such as pharmaceutical tablets and human blood serum.

$3.9. \ \textit{Performance evaluation of the present method}$

The current method using poly(ARS)/GCE was evaluated against recently published approaches, considering factors like linear range, limit of detection (LoD), and the affordability and accessibility of the surface modifier utilized (Table 6).

The method described here, utilizing poly(ARS)/GCE, demonstrated the broadest linear range and the lowest limit of detection compared to previously reported techniques (Table 6). Consequently, the poly(ARS) film, derived from the readily available alizarin red S monomer, exhibited superior performance over methods that relied on more expensive electrode modifiers.

4. Conclusion

This study successfully developed and validated an electrochemical method for the sensitive and selective determination of paracetamol (PCT) using an alizarin red S-modified glassy carbon electrode (poly (ARS)/GCE). The modification significantly enhanced the electrode's electrochemical performance, increasing its active surface area, conductivity, and antifouling properties. The optimized electrode exhibited excellent analytical capabilities, including a broad linear range (0.01–250.0 μM), an ultralow detection limit (1.0 nM), and high reproducibility.

Application of the method to pharmaceutical tablets and human serum samples demonstrated its accuracy and reliability, with recovery rates ranging from 98.8 % to 100.3 % and negligible interference from common coexisting substances. Furthermore, the method's stability and cost-effectiveness highlight its potential for routine quality control and clinical analysis. Compared to previously reported approaches, the poly (ARS)/GCE method offers superior performance and practicality, making it a valuable tool for pharmaceutical and biomedical applications.

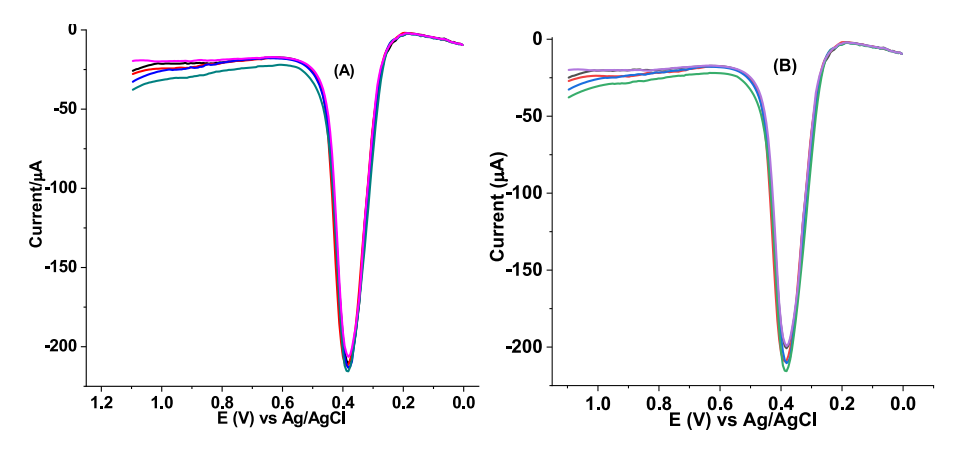


Fig. 14. Five repetitive SWVs of poly(ARS)/GCE in 1.0 mM PCT (pH 7.0 PBS) recorded (A) at every two hrs in one day, (B) at every four days in twenty days' time under the optimized method parameters.

 Table 6

 Performance of the present method compared with previously reported works.

Substrate	Modifier	Method	Dynamic range (μM)	LoD (μM)	Ref.
		HPLC	15.0-300.0	0.01	[3]
SPCE	NanoMIP	DPV	100.0-1000.0	50.0	[25]
GCE	Fe ₃ O ₄ /rGO/Nafion	ASVDPV	2.0-10.0	0.17	[10]
GCE	Au-PEDOT/rGO	CV	0.001-8000.0	0.007	[26]
		LC-MS	0.827-330.77	0.827	[27]
		UV-Vis	5.0-50.0	1.162-10.789 & 0.225-8.955	[28]
CPE	AQMCPE	SWV	33.1-992.2	0.13	[29]
GCE	AgNP/ xGnPs	SWV	4.98-3.38	0.085	[30]
GCE	Sm ₂ O ₃ @ZrO ₂ /CNT	SWV	0.021-15.0	0.00631	[31]
GCE	fCNTs/ZnO/fCNTs	SWASV	2.5-143	0.6	[32]
GCE	Poly(ARS)	SWV	0.01-250.0	0.001	This work

CRediT authorship contribution statement

Wudneh Girum: Writing – review & editing, Writing – original draft, Validation, Software, Resources, Methodology, Investigation, Formal analysis, Data curation. **Adane Kassa:** Writing – review & editing, Writing – original draft, Validation, Supervision, Software, Resources, Methodology, Investigation, Formal analysis, Data curation, Conceptualization.

Author statement

Dr. Adane Kassa is an assistant professor in the Department of Chemistry at Debre Markos University, Ethiopia. He holds an MSc in Inorganic Chemistry and a PhD in Analytical Chemistry, both from Bahir Dar University. His research focuses on catalysis, the development of electrochemical sensors and biosensors, the applications of nanomaterials and metal complexes, pharmaceutical drug analysis, and the detection of heavy metals in environmental samples. Dr. Kassa has authored over 40 articles in reputable journals, with many emphasizing electrochemical methods for analyzing electroactive pharmaceutical compounds. Additionally, he has reviewed more than 20 articles for leading publishers, including Elsevier, Springer, Wiley, and ACS journals. He also serves as an Associate Editor for the *Advanced Journal of Interdisciplinary Studies*.

Wudneh Girum, who earned his MSc in Analytical Chemistry from Debre Markos University in Ethiopia, currently serves as an teacher in the Department of Chemistry at Government High School.

Declaration of competing interest

The authors declare that they have no known competing financial interests or personal relationships that could have appeared to influence

the work reported in this paper.

Acknowledgements

The authors gratefully acknowledge the College of Natural and Computational Sciences, Debre Markos University; the Department of Chemistry, Bahir Dar University; and Tibebe Ghion Hospital, Bahir Dar for providing blood serum samples and laboratory facilities.

Data availability

No data was used for the research described in the article.

References

- A. Kassa, M. Amare, Electrochemical determination of paracetamol, rutin and sulfonamide in pharmaceutical formulations by using glassy carbon electrode–a review, Cogent Chem. 5 (1) (2019) 1681607.
- [2] I. Sadok, K. Tyszczuk-Rotko, New, simple and sensitive voltammetric procedure for determination of paracetamol in pharmaceutical formulations, Insights Anal. Electrochem. 1 (1) (2015).
- [3] C. Engin, S. Yilmaz, G. Saglikoglu, S. Yagmur, M. Sadikoglu, Electroanalytical investigation of paracetamol on glassy carbon electrode by voltammetry, Int. J. Electrochem. Sci. 10 (2) (2015) 1916–1925.
- [4] N. Aminu, S.Y. Chan, N.H. Khan, A.B. Farhan, M.N. Umar, S.M. Toh, A simple stability-indicating HPLC method for simultaneous analysis of paracetamol and caffeine and its application to determinations in fixed-dose combination tablet dosage form, Acta Chromatogr. 31 (2) (2019) 85–91.
- [5] N.R. Ahmad, F.K. Omar, HPLC method for determination of paracetamol in pharmaceutical formulations and environmental water samples, World J. Pharmaceut. Res. 7 (15) (2018) 1–10.
- [6] C. Pasha, Determination of paracetamol in pharmaceutical samples by spectrophotometric method, Eclética Química 45 (3) (2020) 37–46.
- [7] S. Gamal, A.A. Mandour, G.G. Mohamed, S.A. Salih, D.A. Ahmed, Simultaneous spectrophotometric determination of recombined sofosbuvir, ledipasvir and paracetamol together as commonly repurposed drugs for COVID-19 treatment, Fut. J. Pharm. Sci. 9 (1) (2023) 71.

- [8] N.A. Abdallah, M.E. Fathy, M.M. Tolba, A.M. El-Brashy, F.A. Ibrahim, Innovative localized surface plasmon resonance sensing technique for a green spectrofluorimetric assay of ketoprofen, paracetamol and chlorzoxazone in pharmaceutical preparations and biological fluids, RSC Adv. 12 (52) (2022) 33540–33551, https://doi.org/10.1039/D2RA04725J.
- [9] M.H. Hasan, M.E. El-sadek, S.M. El-Adl, The using of dansyl chloride for novel spectrofluorimetric determination of paracetamol in tablet dosage form, Anal. Chem. Lett. 11 (3) (2021) 427–436, https://doi.org/10.1186/s43094-023-00519-8
- [10] N.T.A. Thu, H.V. Duc, N. Hai Phong, N.D. Cuong, N.T.V. Hoan, D. Quang Khieu, Electrochemical determination of paracetamol using Fe3O4/reduced grapheneoxide-based electrode, J. Nanomater. 2018 (1) (2018) 7619419, https://doi.org/ 10.1155/2018/7619419.
- [11] P. Deng, J. Feng, J. Xiao, Y. Wei, X. Liu, J. Li, Q. He, Application of a simple and sensitive electrochemical sensor in simultaneous determination of paracetamol and ascorbic acid, J. Electrochem. Soc. 168 (9) (2021) 096501.
- [12] M. Li, W. Wang, Z. Chen, Z. Song, X. Luo, Electrochemical determination of paracetamol based on au@ graphene core-shell nanoparticles doped conducting polymer PEDOT nanocomposite, Sensors Actuators B Chem. 260 (2018) 778–785.
- [13] W. Boumya, N. Taoufik, M. Achak, N. Barka, Chemically modified carbon-based electrodes for the determination of paracetamol in drugs and biological samples, J. Pharmaceut. Anal. 11 (2) (2021) 138–154.
- [14] S. Cheemalapati, S. Palanisamy, V. Mani, S.M. Chen, Simultaneous electrochemical determination of dopamine and paracetamol on multiwalled carbon nanotubes/ graphene oxide nanocomposite-modified glassy carbon electrode, Talanta 117 (2013) 297–304
- [15] N.S. Prinith, J.G. Manjunatha, N. Hareesha, Electrochemical validation of L-tyrosine with dopamine using composite surfactant modified carbon nanotube electrode, J. Iran. Chem. Soc. 18 (12) (2021) 3493–3503.
- [16] Y.N. Patil, M.B. Megalamani, J.C. Abbar, S.T. Nandibewoor, Investigating hazardous 4-aminoantipyrine with functionalized eco-friendly Fe3O4 nanoparticles decorated nontoxic molybdenum disulfide nanosheet sensor, Results Chem. 6 (2023) 101125.
- [17] A.J. Bard, L.R. Faulkner, Electrochemical Methods: Fundamentals and Applications, 2nd ed., Wiley, New York, 2001.
- [18] A. Kassa, A. Abebe, G. Tamíru, M. Amare, Synthesis of a novel [diresorcinate-1, 10-phenanthrolinecobalt (II)] complex, and Potentiodynamic fabrication of poly (DHRPCo)/GCE for Selective Square wave Voltammetric determination of procaine penicillin G in pharmaceutical and biological fluid samples, ChemistrySelect 7 (1) (2022) e202103458, https://doi.org/10.1002/slct.202103458.
- [19] V. Haridas, Z. Yaakob, S. Sugunan, B.N. Narayanan, Selective electrochemical determination of paracetamol using hematite/graphene nanocomposite modified electrode prepared in a green chemical route, Mater. Chem. Phys. 263 (2021) 124379
- [20] A. Kassa, A. Abebe, M. Amare, Synthesis, characterization, and electropolymerization of a novel cu (II) complex based on 1, 10-phenanthroline for electrochemical determination of amoxicillin in pharmaceutical tablet formulations, Electrochim. Acta 384 (2021) 138402, https://doi.org/10.1016/j. electacta.2021.138402.

- [21] M.S. Jahan, M.J. Islam, R. Begum, R. Kayesh, A. Rahman, A study of method development, validation, and forced degradation for simultaneous quantification of paracetamol and ibuprofen in pharmaceutical dosage form by RP-HPLC method, Anal. Chem. Insights 9 (2014) 75, https://doi.org/10.4137/aci.s18651.
- [22] A.A. Shalaby, A.A. Mohamed, Determination of acid dissociation constants of alizarin red S, methyl orange, bromothymol blue and bromophenol blue using a digital camera, RSC Adv. 10 (19) (2020) 11311–11316.
- [23] Z.D. Leve, N. Jahed, N.A. Sanga, E.I. Iwuoha, K. Pokpas, Determination of paracetamol on electrochemically reduced graphene oxide–antimony nanocomposite modified pencil graphite electrode using adsorptive stripping differential pulse voltammetry, Sensors 22 (15) (2022) 5784, https://doi.org/ 10.3300/c/20155784
- [24] A. Debalkie, A. Guadie, A. Kassa, M. Tefera, Selective determination of norfloxacin in pharmaceutical formulations and human urine samples using poly (8aminonaphthaline-2-sulfonic acid)-modified glassy carbon electrodes, ACS Omega 8 (29) (2023) 25758–25765, https://doi.org/10.1021/acsomega.3c00805.
- [25] K. Alanazi, A.G. Cruz, S. Di Masi, A. Voorhaar, O.S. Ahmad, T. Cowen, E. Piletska, N. Langford, T. Coats, M. Sims, S.A. Piletsky, Disposable paracetamol sensor based on electroactive molecularly imprinted polymer nanoparticles for plasma monitoring, Sensors Actuators B Chem. 329 (2021) 129128, https://doi.org/ 10.1016/j.snb.2020.129128.
- [26] N. Mekgoe, N. Mabuba, K. Pillay, Graphic carbon nitride-SilverPolyvinylpyrrolidone nanocomposite modified on a glassy carbon electrode for detection of paracetamol, Front. Sens. 3 (2022) 827954, https://doi.org/ 10.3389/fsens.2022.827954.
- [27] R.K.T. Kam, M.H.M. Chan, H.T. Wong, A. Ghose, A.M. Dondorp, K. Plewes, J. Tarning, Quantitation of paracetamol by liquid chromatography—mass spectrometry in human plasma in support of clinical trial, Future Sci. OA 4 (8) (2018) FSO331, https://doi.org/10.4155/fsoa-2018-0039.
- [28] K.F. Alsamarrai, S.T. Ameen, Simultaneous ratio derivative spectrophotometric determination of paracetamol, caffeine and ibuprofen in their ternary form, Baghdad Sci. J. 19 (6) (2022) 1276, https://doi.org/10.21123/bsj.2022.6422.
- [29] M. Amare, W. Teklay, Voltammetric determination of paracetamol in pharmaceutical tablet samples using anthraquinone modified carbon paste electrode, Cogent Chem. 5 (1) (2019) 1576349, https://doi.org/10.1080/ 23312009.2019.1576349.
- [30] F. Zamarchi, I.C. Vieira, Determination of paracetamol using a sensor based on green synthesis of silver nanoparticles in plant extract, J. Pharm. Biomed. Anal. 196 (2021) 113912, https://doi.org/10.1016/j.jpba.2021.113912.
- [31] T. Teker, M. Aslanoglu, Sensitive and selective determination of paracetamol using a composite of carbon nanotubes and nanoparticles of samarium oxide and zirconium oxide, Microchem. J. 158 (2020) 105234, https://doi.org/10.1016/j. microc.2020.105234.
- [32] T. Kokab, A. Shah, M.A. Khan, M. Arshad, J. Nisar, M.N. Ashiq, M.A. Zia, Simultaneous femtomolar detection of paracetamol, diclofenac, and orphenadrine using a carbon nanotube/zinc oxide nanoparticle-based electrochemical sensor, ACS Appl. Nano Mater. 4 (5) (2021) 4699–4712, https://doi.org/10.1021/ acsapm_1c00310